CHEMICAL ENGINEERING TRANSACTIONS
VOL. 72, 2019

A publication of AIDIC
The Italian Association of Chemical Engineering
Online at www.aidic.it/cet

Guest Editors: Jeng Shiun Lim, Azizul Azri Mustaffa, Nur Nabila Abdul Hamid, Jiří Jaromír Klemeš

ISBN 978-88-95608-69-3; **ISSN** 2283-9216
DOI: 10.3303/CET1972030

Adsorption and Desorption of Nickel (II) Ion by Oil Palm Empty Fruit Bunch grafted Polyvinyl Alcohol Hydrogel

Mohamed Rizwan Rafeek[a], Nurul Ekmi Rabat[b,*], Wan Zaireen Nisa Yahya[b], Musliha Abdul Ghani[a]

[a]Department of Chemical Engineering, Universiti Teknologi PETRONAS, 32610, Bandar Seri Iskandar, Perak, Malaysia
[b]Institute of Contaminant Management, Universiti Teknologi PETRONAS, 32610, Bandar Seri Iskandar, Perak, Malaysia
nurulekmi.rabat@utp.edu.my

Oil palm empty fruit bunch grafted polyvinyl alcohol (OPEFB-*g*-PVA) hydrogel was prepared for the removal of Nickel (II) ions in wastewater. OPEFB-*g*-PVA was synthesized using ammonium persulfate (APS) as the initiator and boric acid as the crosslinking agent via solution polymerization. Atomic absorption spectroscopy (AAS) was used to determine Ni (II) adsorption properties and scanning electron microscope (SEM) was used to study the morphology. Langmuir and Freundlich isotherms were used to analyse the adsorption mechanism. The most efficient hydrogel in Ni (II) adsorption was obtained at 15 wt% OPEFB-g-PVA hydrogel as the concentration of Ni (II) reduced from 10 mg/g to 7.00 ± 0.02 mg/g with the highest water absorbency capacity at 134 g/g. For desorption of Ni (II), 20 wt% OPEFB-g-PVA hydrogel shows the highest amount of Ni (II) desorption concentration of 2.48 mg/g. The adsorption isotherms fit the linear Langmuir isotherm model for OPEFB filled hydrogels. This low-cost sorbent based OPEFB proved to have a great future potential in wastewater treatment.

1. Introduction

In recent years, heavy metal presences in water is well acknowledged to be extremely harmful to majority of living organisms. Nickel (II) especially, exceeding its critical level might cause about serious lung and kidney problems, gastrointestinal distress, pulmonary fibrosis and skin dermatitis. And it is known that nickel is human carcinogen. Indeed, heavy metals pollution in wastewater has become one of the most serious environmental issues and a worldwide concern (Ayucitra et al., 2017). Various methods were used in heavy metal removal from wastewater including precipitation (Bratskaya et al., 2009), reverse osmosis (Jeppesen et al., 2009), ion-exchange (Verma et al., 2008), ultra-filtration (Barakat and Schmidt, 2010) and adsorption (Kow et al., 2017). However, adsorption is the most appropriate method due to its characteristic of great efficiency and easiness to remove the heavy metals from wastewater.

Biosorption is a cost-effective process where existing adsorbent is improved by adding agriculture waste during the production. Biosorption of heavy metals from aqueous solutions has proven very promising in the removal of contaminants from aqueous effluents as this biosorption technology able to reduce the concentration of heavy metal ions to very low concentration with the use of inexpensive biosorbent materials (Demirbas, 2008). As a waste product, oil palm empty fruit bunch fibre (OPEFB) is readily available, renewable and the cheapest among all biodegradable natural polymers. OPEFB fibre is obtained after the extraction of oil from the fruit bunch by stripping off the fruits is done (Wen et al., 2017). The addition of OPEFB in an adsorbent has improved the strength by enhancing the fibre matrix adhesion in the adsorbent and providing rougher surface. (Yaacob et al., 2014). Swelling caused by water absorbency capacity of fibres has a strong impact on adsorption properties. The bigger the amount of water absorbency gives bigger swelling and increase the heavy metals adsorption (Demirbas, 2008).

Hydrogel is a water-swollen and cross-linked polymeric network that is produced by a polymerization reaction of one or more hydrophilic monomers. It exhibits the capacity to swell and retain a high amount of water within its structure and will not dissolve in water (Zohuriaan-Mehr and Kabiri, 2008). PVA hydrogels are non-carcinogenic, non-toxic and easy to process. One of the interesting characteristics of PVA hydrogels is it has

Paper Received: 30 March 2018; Revised: 03 August 2018; Accepted: 21 November 2018

Please cite this article as: Rafeek M.R., Rabat N.E., Nisa Yahya W.Z., Abdul Ghani M., 2019, Adsorption and desorption of nickel (ii) ion by oil palm empty fruit bunch grafted polyvinyl alcohol hydrogel, Chemical Engineering Transactions, 72, 175-180 DOI:10.3303/CET1972030

high degree of swelling when immersed in water while maintaining its elastic and rubbery texture. PVA as a commercial industrial product, is highly valued for its biodegradability and solubility properties (Jin and Bai, 2002). From multiple researches conducted on PVA hydrogels, it is proven that it has a faster adsorption kinetics in removing heavy metals from aqueous solution (Jamnongkan and Singcharoen, 2016). Thus, the major purpose and aim of this project is to study the Nickel (II) adsorption and desorption mechanism of OPEFB-*g*-PVA hydrogel. The main materials used in this project were oil palm empty fruit bunch, gelatine and PVA. Hydrogel was prepared using solution polymerization technique. This hydrogel was then tested for adsorption and desorption mechanism in Nickel (II) removal from an aqueous solution. The sample was characterized by using atomic absorption spectroscopy, scanning electron microscope, and the water absorption capacity. The adsorption mechanism of the hydrogel was determined by using Langmuir and Freundlich isotherms.

2. Materials and method

2.1 Synthesis of PVA-*g*-OPEFB hydrogel

Polyvinyl alcohol (PVA) was synthesized by dissolving 44 g PVA powder in distilled water at 90 °C for 1 h with constant stirring. The solution was left to cool at room temperature for 30 min. A 20 mL of the aqueous solution of PVA was then added to a beaker before immersed in a water bath at 70 °C. A 3 M solution of sodium borate (BORAX) was prepared by neutralization of boric acid and sodium hydroxide. The desired amount of OPEFB (size: 150 μm) powder were added to the PVA solution and stirred. Once the solution becomes homogenous, 5 mL of sodium borate was added to the solution. The required amount of initiator, ammonium persulfate (APS) was then added to the PVA solution. At the end of the reaction, the flask was cooled under running tap water. The crude product was filtered, washed with distilled water and purified with acetone. The hydrogel was dried in a drying oven at 70 °C to constant weight. The experiment was repeated for ranges of the OPEFB weight percent of 0 %, 5 %, 10 %, 15 % and 20 %.

2.2 Water absorbency capacity (WAC)

Water absorption capacity of each OPEFB-*g*-PVA hydrogels were tested to determine the swelling properties of all adsorbents. The mass of dried sample was recorded and the sample was immersed in water for 24 hours. The surface water from the water-swollen hydrogel was removed by using a soft tissue paper before the mass of water-swollen hydrogel was recorded (Sutradhar et al. 2015).
The WAC was determined by using Eq(1).

$$WAC = \frac{Mass\ of\ sample\ immersed\ in\ water\ (g) - Mass\ of\ dried\ sample\ (g)}{Mass\ of\ dried\ sample\ (g)} \times 100 \quad (1)$$

2.3 Scanning electron microscope (SEM)

The SEM photographs of the surfaces of OPEFB-g-PVA hydrogel were taken using a scanning electron microscope (SEM) model JEOL JSM-6390LV (USA). A small portion of the sample was mounted on the copper stub and sputter-coated with a thin layer of gold in a plasma chamber for a few minutes. The coated-sample was properly mounted onto SEM stage in the chamber, and then it was vacuum for several minutes. Followed by set the electron at voltages of 5 kV – 10 kV, in which higher voltage performed better resolution.

2.4 Nickel(II) adsorption on OPEFB-*g*-PVA hydrogel

2.4.1 Adsorption

Hydrogel was tested in an aqueous solution with the presence of Nickel (II) in the range of 0-10 mg/g. Adsorption of Ni (II) in the hydrogel was setup as in Figure 1a, monitored, and the sample from the aqueous solution was taken every 2 h for the period of 8 h. The change in the concentration over time for the period of 8 h was obtained.

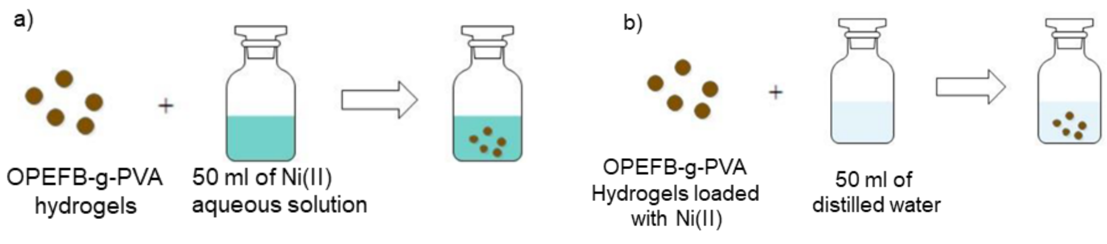

Figure 1: Schematic diagram of Ni (II) (a) adsorption and (b) desorption on the surface of hydrogels.

2.4.2 Desorption

Desorption of Ni (II) by concentration difference from the hydrogel was observed, and the reading of Ni (II) concentration in distilled water as in Figure 1b. The sample of distilled water was taken every 2 h for the period of 8 h. Concentrations of Ni (II) in the solution for both experiments were characterized by using Atomic Absorption Spectroscopy (AAS) model Hitachi Z-5000 Polarized Zeeman Atomic Absorption Spectrophotometer.

2.5 Isotherms studies

Langmuir and Freundlich isotherms were utilized to study the Ni (II) adsorption capacity of OPEFB-g-PVA hydrogel. The assumptions of Langmuir isotherm model are that the surface of OPEFB-*g*-PVA is homogenous and the adsorption potential towards Ni (II) is always constant. While Freundlich isotherm model is an empirical equation assuming that the adsorption process takes place on heterogeneous surfaces. Langmuir and Freundlich isotherm models are represented in Eq(2) and Eq(3).

$$\frac{1}{q_e} = \frac{1}{k_L Q_m}\frac{1}{c_e} + \frac{1}{Q_m} \quad (2)$$

$$\ln q_e = \frac{1}{n}\ln c_e + \ln K_F \quad (3)$$

q_e is the amount of Ni (II) adsorbed at equilibrium (mg/g), k_L is Langmuir constant (L/mg), Q_m is the maximum adsorption at monolayer (mg/g) and c_e is the equilibrium concentration (mg/L). K_F and 1/n are the Freundlich characteristic constants, indicating adsorption capacity and adsorption intensity. The value of q_e can be determined by using the Eq(4).

$$qe = \frac{change\ in\ concentration\ (mg/L)\ \times volume\ of\ solution\ (L)}{mass\ of\ adsorbent(g)} \quad (4)$$

3. Result and discussions

3.1 Water absorptions capacity (WAC)

Water absorptions capacity of all the samples were determined and calculated. The result is tabulated in the Table 1. WAC of OPEFB-*g*-PVA hydrogel has increased with the increasing amount of OPEFB from 0 wt% to 15 wt%. The highest WAC was achieved by 15 wt% OPEFB-*g*-PVA hydrogel.

This can be related to the highly hydrophilic nature of the OPEFB fibre as they are in abundance with hydroxyl group. Besides, OPEFB also acted as the physical cross-linking agent to accommodate more water inside the hydrogel structure (Liang et al. 2009). High WAC constitutes high volumes of water-swollen hydrogel which also increases the surface area of adsorbent, providing more space for Ni (II) to be attached on the surface of the hydrogel.

Table 1: Water absorption capacity of different wt% of OPEFB

Amounts of OPEFB (wt%)	Water absorbency of the hydrogels (%)
0	126
5	129
10	131
15	134

3.2 Scanning electron microscope (SEM)

Surface morphologies of the hydrogels was studied by using scanning electron microscope (SEM). The purpose of this is to identify surface morphologies and analyse the microstructure of the hydrogels. For different weight percent of OPEFB in OPEFB-*g*-PVA, different surface morphology was observed. Commonly, a highly porous condition of hydrogel is observed for all OPEFB-*g*-PVA hydrogels. Figure 2 shows the surface morphology of OPEFB-g-PVA hydrogels from 0 wt to 15 wt%.

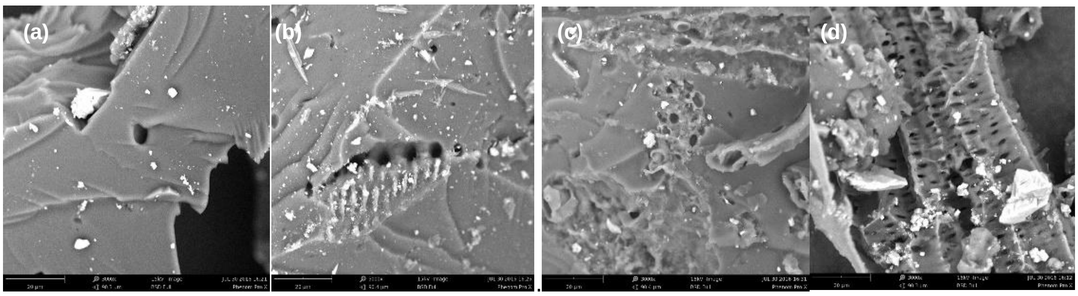

Figure 2: SEM Images (3000x magnification) showing porous structure of OPEFB-g-PVA hydrogel (a) 0 %; (b) 5 %; (c) 10 % and (d) 15 %.

Porous structures can be well observed in 15 wt% OPEFB-*g*-PVA hydrogel compared to other hydrogels. For 0% OPEFB-g-PVA hydrogel in Figure 3a, the porous body is less compared to the others. This is due to the absence of OPEFB fibres which increases the porosity to absorb more water.
As the weight percent of OPEFB is increased from 5 % to 15 %, more porous structures can be observed. However, for 15 wt. % of OPEFB, the porous structure is more and aligned accordingly. This shows that the 15 wt. % OPEFB is the best structure for absorbing more water. The SEM images are aligned with WAC values in Table 1.

3.3 Adsorption and desorption of nickel ion

The adsorption and desorption of the Nickel (II) by all different wt% OPEFB-*g*-PVA hydrogels were determined and shown in Figure 3. Comparing to 0 wt% OPEFB-*g*-PVA hydrogel, the adsorption mechanism of all the other hydrogels were more efficient. Adsorbent made of 10 wt%, 15 w%, and 20 wt% OPEFB-*g*-PVA hydrogels have the highest Nickel (II) adsorptions.
The adsorption amount of 5 wt% OPEFB-*g*-PVA was slightly lowered due to the lack of OPEFB fibre in the hydrogel. This result indicates that the presences of OPEFB fibre increases the Ni (II) adsorption efficiency of hydrogel and in agreement with other researches (Jamnongkan and Singcharoen, 2016). From the Figure 4b, the 20 wt% OPEFB-g-PVA hydrogel also shows the highest amount of Nickel (II) desorption at 2.48 mg/g.
The desorption mechanisms of the 10 wt% and 15 wt% OPEFB-g-PVA hydrogels are more efficient due to the high water absorbing capacity which leads to the hydrogel to desorb Nickel (II). The desorption mechanism occurs by the concentration difference of the immersing solution (Lam et al., 2016).

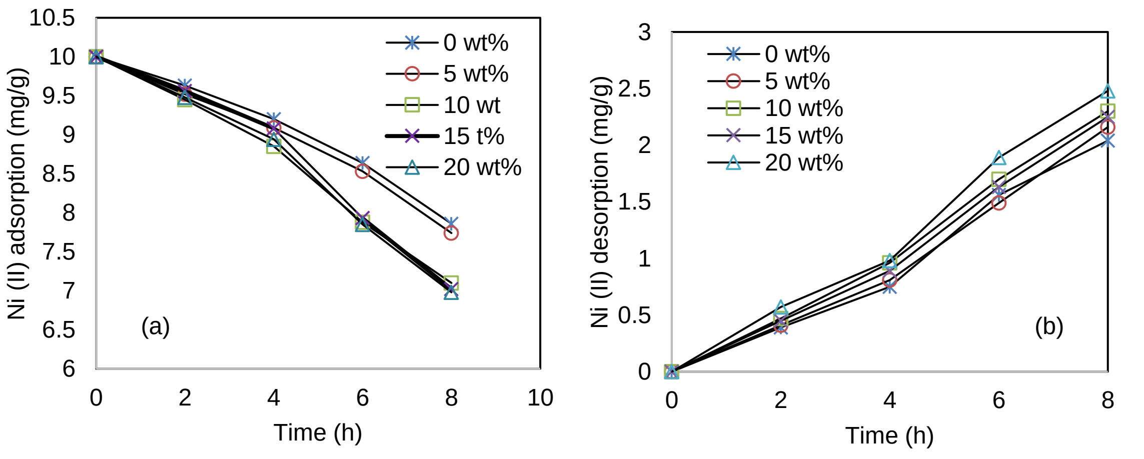

Figure 3: (a) Adsorption and (b) desorption of Ni (II) ions by OPEFB-g-PVA hydrogels.

3.4 Isotherm studies

Figures 4 shows the initial concentration of Ni(II) versus equilibrium adsorption capacity of all hydrogels with 0 wt% , 10 wt and 20 wt% OPEFB together with the Langmuir and Freundlich models. All hydrogels have the same behavior where their equilibrium adsorption capacity increases with the initial concentrations. Hydrogels with abundant amount of OPEFB are best fitted with Langmuir model while hydrogel without OPEFB is best fitted with Freundlich model.

Langmuir and Freundlich isotherms for Ni (II) adsorption of all OPEFB-*g*-PVA hydrogels were also calculated and the results are summarized in Table 2. The q_m values in Langmuir isotherm gave the maximum adsorption amount of Nickel (II) on hydrogels. It was recorded that the 10 wt% OPEFB-*g*-PVA adsorbent acquired the highest Ni (II) adsorption capacity at 121.95 mg/g.

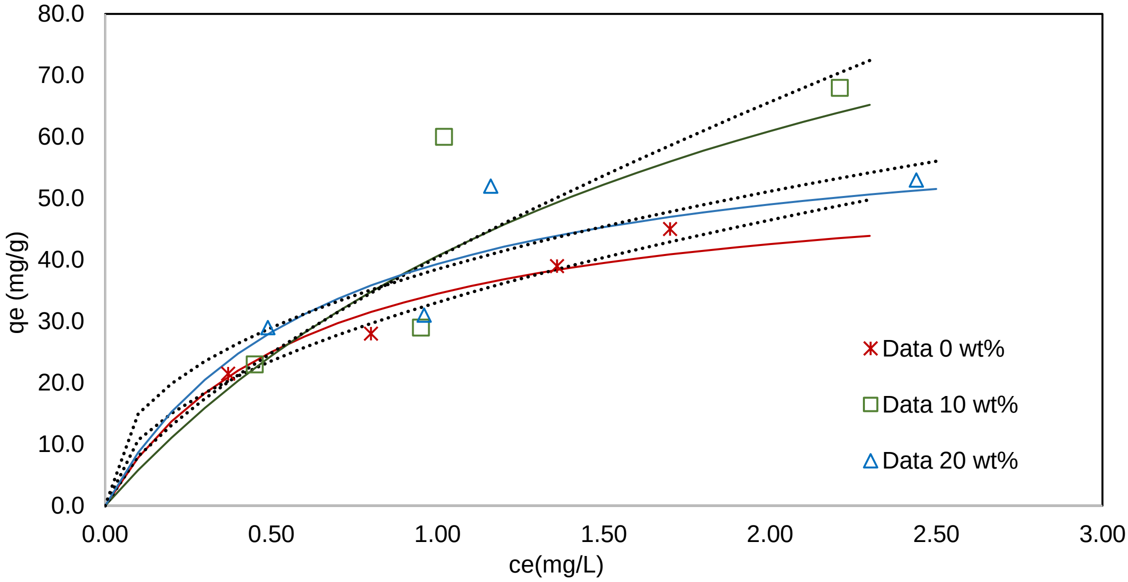

Figure 4: Amount of Ni (II) adsorbed at equilibrium (mg/g) versus equilibrium concentration of all hydrogels (the solid line represents Langmuir model, the dashed line represents Freundlich model).

Based on Table 2, Freundlich constant (1/n) is represented as the adsorption intensity of the adsorbent. The adsorption is excellent when the value of 1/n lies around $0.1 < 1/n \leq 0.5$, Ni (II) is easy to adsorb when the value of 1/n is $0.5 < 1/n \leq 1$, and difficult to adsorb when value of $1/n > 1$ (Tang et al., 2014). The 1/n values of all hydrogels lied in the range from 0.5 to 0.1 except for 10 wt% OPEFB-*g*-PVA indicating that Nickel (II) could be easily adsorbed on the all hydrogels.

Table 2: Langmuir and Freundlich parameters for Nickel (II) ions adsorption on OPEFB-g-PVA.

Amount of OPEFB in hydrogels (wt%)	Langmuir Parameters			Freundlich Parameters		
	q_m (mg/g)	K_L	R^2	1/n	K_F	R^2
0	55.56	1.64	0.94	0.49	33.11	0.97
5	61.73	1.09	0.96	0.50	29.96	0.98
10	121.95	0.50	0.76	0.70	40.44	0.73
15	90.09	0.78	0.72	0.53	36.60	0.65
20	64.94	1.54	0.68	0.41	38.50	0.67

By using the correlation coefficient, R^2 it can be seen that the adsorptive behavior of Ni (II) on 10 wt%– 20 wt% OPEFB filled hydrogels was better fitted by Langmuir equation while 0 wt% - 5 wt% are better fitted by Freundlich model. This indicates that Ni (II) ions adsorbed on OPEFB filled hydrogel as a monolayer adsorption. However, the R^2 decreases as the amount of OPEFB in hydrogel increases. Langmuir isotherm model assumes the formation of a monolayer on a structurally homogeneous sorbent surface in which there is no interaction among the adsorbed molecules. With the addition of more OPEFB, the homogeneous structure is disturbed.

4. Conclusions

Oil palm empty fruit bunch grafted polyvinyl alcohol (OPEFB-g-PVA) was prepared at different weight percent of OPEFB fibre from 0 to 20 wt%. The chelating ability of OPEFB-g-PVA was evaluated based on the removal of Nickel (II) in aqueous solution. A highly porous structure of the OPEFB-g-PVA hydrogel was obtained from

SEM images for 15 wt% OPEFB-g-PVA. The water absorption capacity (WAC) was at the highest at 134 % for 15 wt% of OPEFB. For Ni (II) adsorption and desorption, the most efficient hydrogel in Nickel(II) adsorption was obtained by 15 wt% and 20 wt% OPEFB-g-PVA hydrogels as the concentration of Nickel reduced from 10 mg/g to 7.00 ± 0.02 mg/g. Langmuir isotherm was recorded to be more suitable for Ni (II) adsorption on OPEFB-*g*-PVA hydrogels.

Acknowledgments

Great appreciations offered to Universiti Teknologi PETRONAS for the facilities and research fund, STIRF 0153AA-F08.

References

Ayucitra A., Gunarto C., Kurniawan V., Hartono S.B., 2017, Preparation and characterization of biosorbent from local robusta spent coffee grounds for heavy metal adsorption, Chemical Engineering Transactions, 56, 1441-1446.

Barakat M.A, Schmidt E., 2010, Polymer-enhanced ultrafiltration process for heavy metals removal from industrial wastewater, Desalination, 256, 90–93.

Bratskaya S.Y., Pestov A.V., Yatluk Y.G., Avramenko V.A., 2009, Heavy metals removal by flocculation/precipitation using N-(2-carboxyethyl)chitosans, Colloids and Surfaces A: Physicochemical and Engineering Aspects, 339, 140–144.

Demirbas A., 2008, Heavy metal adsorption onto agro-based waste materials: A review. Journal of Hazardous Materials, 157, 220–229.

Jamnongkan T., Singcharoen K., 2016, Towards Novel Adsorbents: The ratio of PVA/Chitosan Blended Hydrogels on the Copper (II) Ion Adsorption, Energy Procedia, 89, 299–306.

Jeppesen T., Shu L., Keir G., Jegatheesan V., 2009, Metal recovery from reverse osmosis concentrate, Journal of Cleaner Production, 17, 703–707.

Jin L., Bai R., 2002. Mechanisms of lead adsorption on chitosan/PVA hydrogel beads, Langmuir, 18, 9765-9770.

Kow K., Kiew P.L., Yusoff R., Abdullah E.C., 2017, Preliminary evidence for enhanced adsorption of cadmium(II) ions using nano-magnetite aligned in silica gel matrix, Chemical Engineering Transactions, 56, 1231-1236.

Lam Y.F., Lee L.Y., Chua S.J., Lim S.S., Gan S., 2016, Insights into the equilibrium, kinetic and thermodynamics of nickel removal by environmental friendly Lansium domesticum peel biosorbent, Ecotoxicology and Environmental Safety, 127, 61–70.

Liang R., Yuan H., Xi G., Zhou Q., 2009, Synthesis of wheat straw-g-poly(acrylic acid) superabsorbent composites and release of urea from it, Carbohydrate Polymers, 77, 181–187.

Sutradhar S.C., Khan M.M.R., Rahman M.M., Dafadar N.C., 2015, The synthesis of superabsorbent polymers from a carboxymethylcellulose/acrylic acid blend using gamma radiation and its application in agriculture, Journal of Physical Science, 26, 23–39.

Tang H., Zhang L., Hu L., Zhang L., 2014, Application of Chitin Hydrogels for Seed Germination, Seedling Growth of Rapeseed, Journal of Plant Growth Regulation, 33, 195–201.

Verma V.K., Tewari S., Rai J.P.N., 2008, Ion exchange during heavy metal bio-sorption from aqueous solution by dried biomass of macrophytes, Bioresource Technology, 99, 1932-1938.

Wen S. J., Rabat N. E., Osman N., 2017, Synthesis and characterization of oil palm empty fruit bunch-grafted -polyvinyl alcohol (OPEFB-g-PVA) hydrogel for removal of copper ions from aqueous solution, AIP Conference Proceedings, 1901(1), DOI: 10.1063/1.5010468

Zohuriaan-Mehr M.J., Kabiri K., 2008, Superabsorbent polymer materials: A review, Iranian Polymer Journal 17, 451–477.